EUVL source optimisation for 13.5 nm operation

Unresolved transition array

In a laser-produced plasma, an unresolved transition array (UTA) can be the strongest feature in an EUV spectra. A UTA generally has too many lines to identify individual transitions; however, both the energy level and spectral distributions can be parameterised statistically [1]. The most intense UTA are observed from n = 4 n = 4 and n = 5 n = 5 transitions.

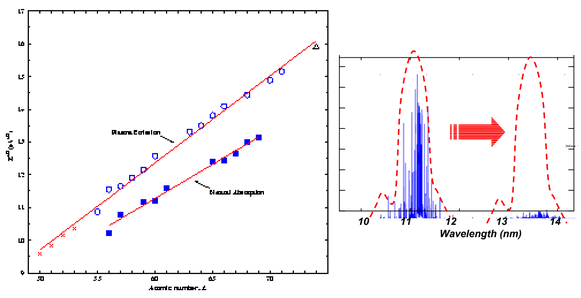

Figure 1 The $4p^64d^n$ - $4p^54d^{n+1}$ + $4d^{n-1}4f$ UTA emission completely dominates the spectrum of xenon and the elements around it. Position depends on Z and essentially follows a Mosely plot. From Z = 54 (Xe) to Z = 50 (Sn), the main UTA band moves from 11 nm to 13.5 nm [2].

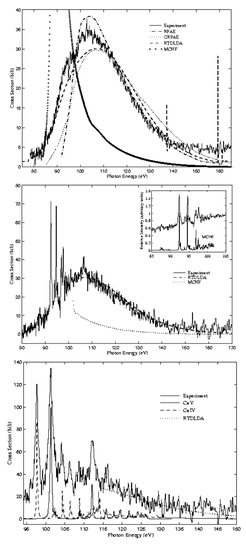

Photoabsorption spectra from Sn through the lanthanides are dominated by 4d f resonances. With increasing ionisation, the 4d f oscillator strength is transferred to the 4d 4f transition.

Figure 2 Transfer of oscillator strength along a Cesium isonuclear sequence [3].

Wavefunction collapse

As the 4f wavefunction collapses, the 4d,4f overlap and oscillator strength increases.

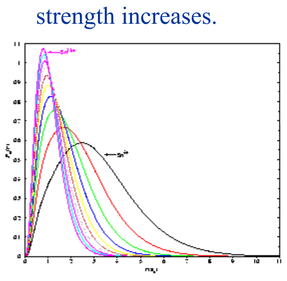

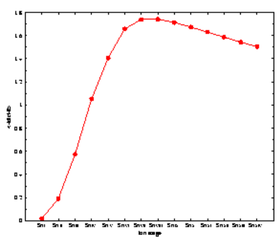

The degree of 4d,4f overlap determines the transition intensity and peaks for ion stages of Sn past Sn^{5+}

Figure 3 4f collapse from Sn^{4+} to Sn^{13+} [4].

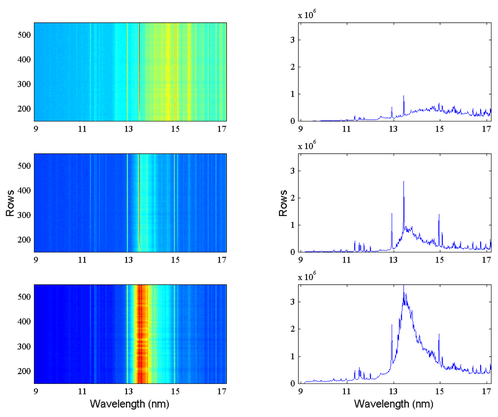

Figure 4 Spectra of Sn at increasing laser power densities (from top) showing increased UTA brightness in 13.5 nm range (ceramic-doped with 6% Sn by number).

Sn steady-state plasma modelling

- Many ion stages contribute to in-band emission (in principle, all stages from Sn^{8+} to Sn^{13+}).
- Emission originates from the n=4 n=4 UTA and is very intense.
- Optimum emission when tin is present as a low percentage impurity.

Steady state collisional-radiative plasma model predicts maximum relative ion populations as a function of temperature [5].

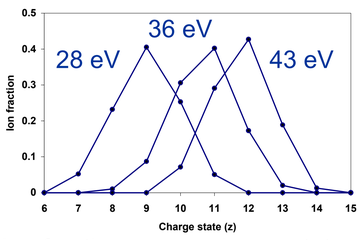

Figure 5 Ion fraction versus charge state for 28 eV, 36 eV, and 43 eV.

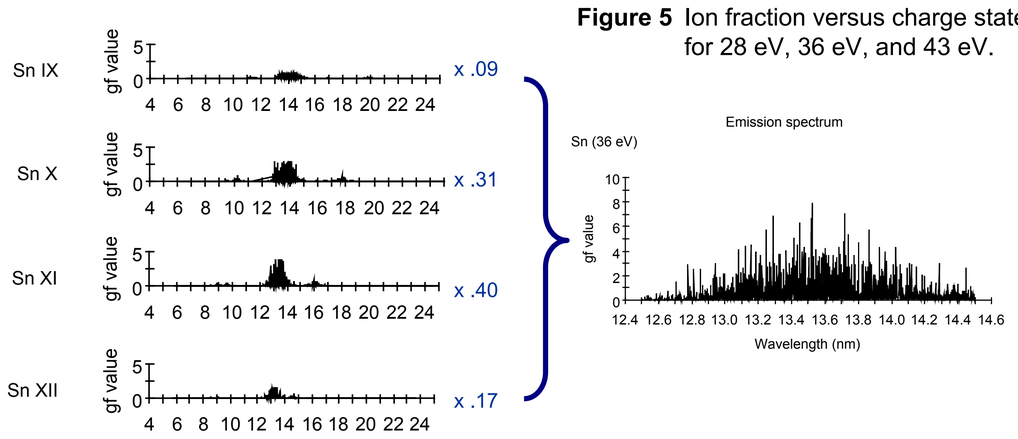

Figure 6 Oscillator strength versus wavelength (nm) of contributing ions (Sn IX, Sn X, Sn XI, Sn XII) for 36 eV plasma (left). Contributing ions weighted by relative ion density population (Sn IX 9%, Sn X 31%, Sn XI 40%, Sn XII 17%) (right).

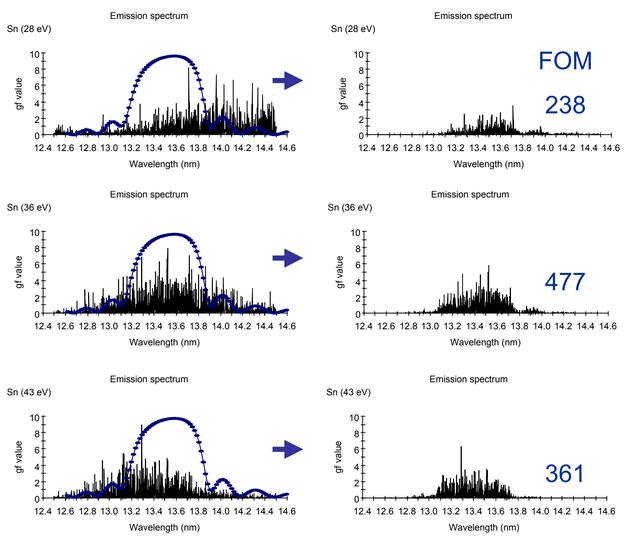

Figure 7 Total oscillator strength versus wavelength (nm) with mirror reflectivity function superimposed (left). In-band oscillator strength versus wavelength (nm) for 28 eV, 36 eV, and 43 eV Sn plasma and FOM (right).

Figure of merit: FOM = $_z$(*gf*(z) f(z)) x R( )

- *gf*(z) = summed oscillator strengths for ion z.
- f(z) = fractional weighting of ion z.
- R( ) = reflectivity of Mo/Si multilayer.

Laser Flux W cm^{-2}	Electron Temp. (eV)	Figure of Merit
4 10^{10}	28.1	238
5 10^{10}	32.2	414
6 10^{10}	35.9	477
7 10^{10}	39.4	439
8 10^{10}	42.7	361

Element mixtures and opacity effects: targets other than Sn

Spectra from metal targets are dominated by continuum emission with some strong emission and absorption lines superimposed. Spectra of dilute targets are dominated by an intense UTA with greatly reduced continuum emission.

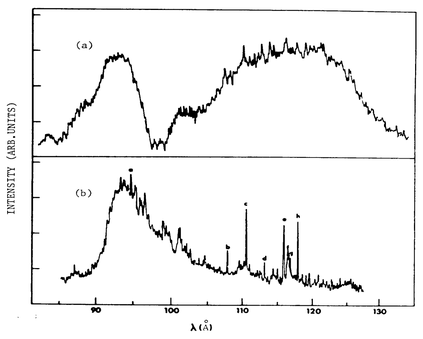

Figure 8 La metal (top), La oxide (bottom) [6].

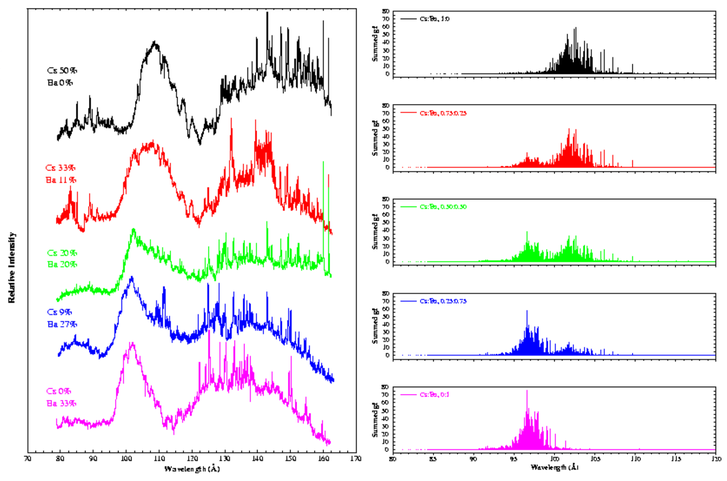

Figure 9 Opacity effects in UTA profile of mixed plasmas by mixing Cs and Ba chloride salts: from 50% Cs and 0% Ba (top) to 0% Cs and 33% Ba (bottom).

Sn targets

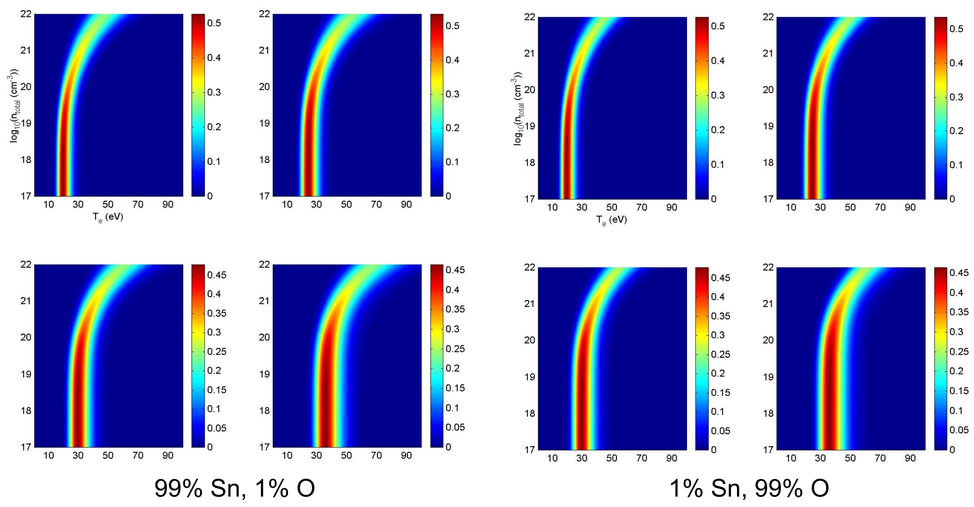

Mixture effect of Sn and O (Sn^{8+} to Sn^{11+}).

Note that the effect of concentration on ion distribution as a function of temperature (and hence laser power) is negligible.

Figure 10 Atomic number density versus electron temperature (eV).

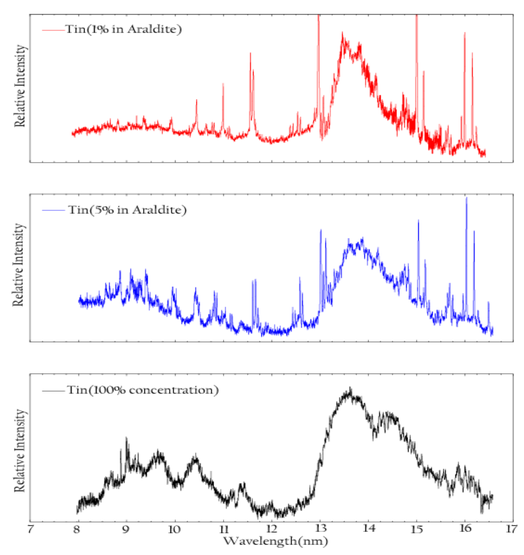

Figure 11 Emission spectra of tin and tin doped araldite targets

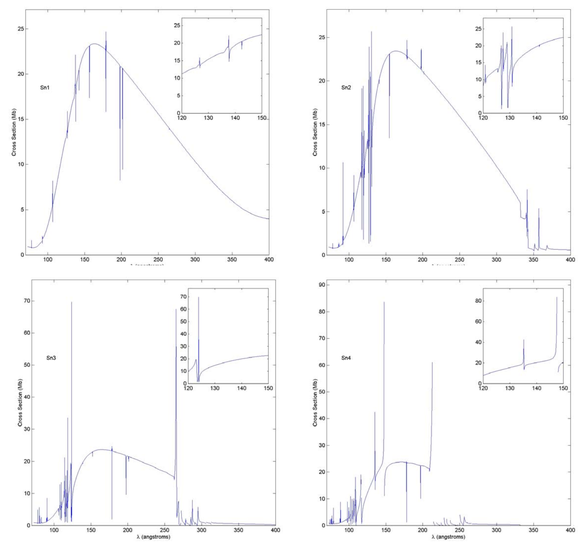

Figure 12 The photoabsorption (excitation and ionization) cross sections of neutral Sn I to Sn IV, calculated using the Relativistic Time Dependent Local Density Approximation (RTDLDA), DAVID [7], showing the influence of continuum absorption in lower ion stages.

Other possible sources

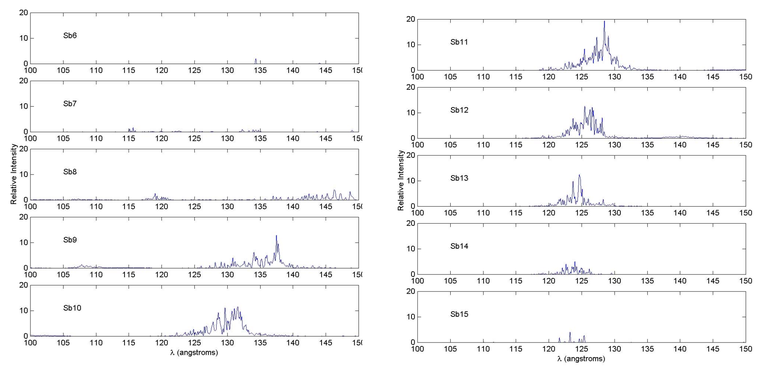

Possible other sources include antimony (FOM = 221 at 28 eV, 285 at 32 eV, 164 at 43 eV). Note that configuration interaction effects are important [8]. Atomic structure calculations are made with the MCHF Cowan code (typically 10% reduction of Slater Condon parameters) [9].

Figure 13 Theoretical spectra for antimony ions from resonance $4p^64d^n$ - $4p^54d^{n+1}$ + $4d^{n-1}(4f + 5p)$ transitions.

References

[1] Bauche-Arnoult and Bauche, "Statistical approach to the spectra of plasmas, *Physica Scripta* T**40**, 58, 1992.
[2] O'Sullivan and Carroll, "4d-4f emission resonances in laser-produced plasmas," *J. Opt. Soc. Am*, **71**, 3, 1981.
[3] Cummings *et al.*, "Wave-function collapse with increasing ionization: 4d photoabsorption of Cs through Cs^{4+}," *Phys. Rev. A* **6303** 2702, 2001.
[4] O'Sullivan and Faulkner, "Tunable narrowband soft x-ray source for projection lithography," *Opt. Eng.* **33**, 3978, 1994.
[5] Colombant and Tonon, "X-ray emission in laser-produced plasmas," *J. Appl. Phys.* **44** (8), 3524–3537, 1973.
[6] Carroll and O'Sullivan, "Ground-state configurations of ionic species I through XVI for Z = 57-74 and the interpretation of 4d-4f emission resonances in laser-produced plasmas," *Phys. Rev.* A, **25**, 1, 1982.
[7] Libermani and Zangwill, *Computer Physics Communications*, **32**, 75, 1984.
[8] Mandelbaum *et al.*, "Interpretation of the quasicontinuum band emitted by highly ionized rare-earth elements in the 70-100 Å range," *Phys. Rev.* A, **35**, 12, 1987.
[9] Cowan, *The theory of atomic spectra and structure*, Berkeley, University of California Press, 1981.

Department of Experimental Physics, University College Dublin, Belfield, Dublin 4, Ireland

Gerry O'Sullivan, Padraig Dunne, Emma Sokell, Anthony Cummings, Nicola Murphy, Kenneth Fahy, Andy Fitzpatrick, Lynn Gaynor, Paddy Hayden, Dariusz Kedzierski, Deirdre Kilbane, Michael Lysaght, Luke McKinney, and John White